Natural Hazards (2023) 116:2245–2268
https://doi.org/10.1007/s11069-022-05762-5

ORIGINAL PAPER

New geologic paleoseismological observations along the Acipayam–Serinhisar fault zone, SW Anatolia

Mete Hancer[1] · **Nebil Kenanoglu**[1] · **Erdal Akyol**[1]

Received: 5 September 2022 / Accepted: 7 December 2022 / Published online: 16 December 2022

Abstract
An earthquake of $M = 5.6$ occurred on the March 20, 2019, in Acipayam, Denizli, located in a seismically active area at the southwest Anatolian fault system, in Türkiye. It caused extensive damages of infrastructures. The relevant fault (Acipayam–Serinhisar fault zone) has not shown on the active fault map of Türkiye, and it has been discovered first time by this study. The earthquake occurred on the Acipayam segment of this fault zone, which is divided into two separate segments. Three trenches were excavated for paleoseismological studies on this segment. The samples collected from the trenches were dated by radiocarbon method. The obtained data proposed three seismic events, which caused a surface rupture, at BC 235–95, AD 1227–1263 and AD 1471–1738. Considering the last two events, this fault segment produced two earthquakes of magnitude 6.0 and 6.5, 350 years apart.

Keywords Acipayam · Active fault · Paleoseismology · Radiocarbon dating · Trench

1 Introduction

Paleoseismological studies are of important for earthquake hazard assessment and enlighten the historical earthquakes. They could help to build earthquakes models of at scales of time and magnitude (Cinti et al. 2021). The Arabian, African and Eurasian plate motions have caused complex tectonic features in Turkiye, and they show different paleoseismological outcomes (Gürboğa and Gökçe 2019). Türkiye is a part of the Anatolian microplate, which may be a porsion of the Eurasian plate (Nyst and Thatcher 2004) as shown in Fig. 1. The southwestern Anatolia is a tectonically active region in the Anatolian microplate. Active continental deformation in the Anatolian microplate is evident, and strike slip deformation and extensional tectonic regime in the plate still continue today

✉ Mete Hancer
mhancer@pau.edu.tr

Nebil Kenanoglu
nblkenanoglu@gmail.com

Erdal Akyol
eakyol@pau.edu.tr

[1] Department of Geological Engineering, Engineering Faculty, Pamukkale University, Denizli, Turkey

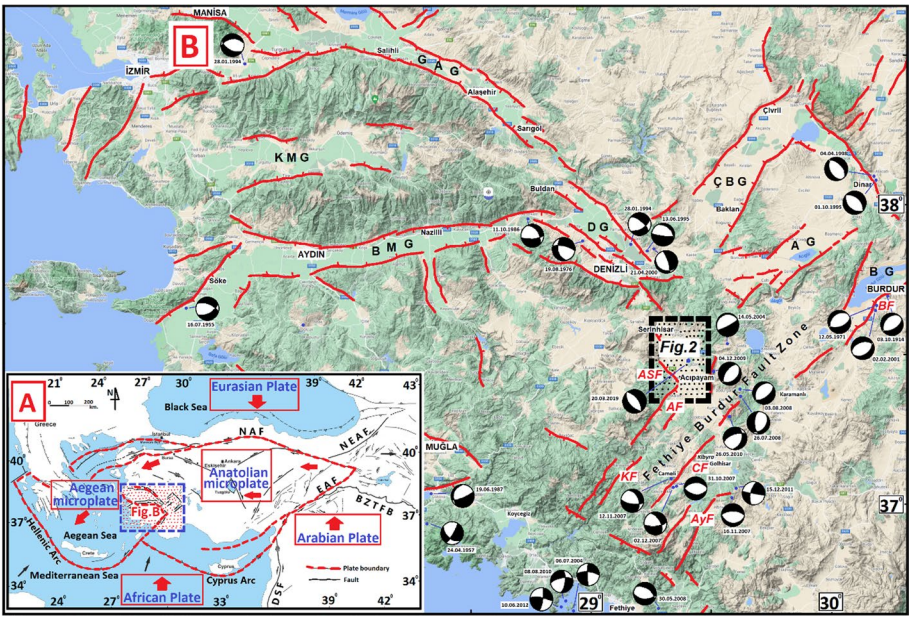

Fig. 1 **A** Location map within the tectonic framework of the Turkey, explanations: NAF: North Anatolian fault, EAF: East Anatolian fault, NEAF: Northeast Anatolian fault, BZTFB: Bitlis-Zagros thrust and fold belt (modified from Nyst and Thatcher 2004; Över et al. 2010; Catlos et al. 2021), **B** morphotectonic active fault map and focal mechanism of the historical earthquakes in SW of Anatolia (Elitez et al. 2016) (on Google Maps). Explanations: BMG: Büyük Menderes graben, KMG: Kücük Menderes graben, GAG: Gediz-Alasehir graben, DG: Denizli graben, ÇBG: Civril-Baklan graben, AG: Acigöl graben, BG: Burdur graben, ASF: Acipayam–Serinhisar fault, AF: Acipayam fault, BF: Burdur fault, AyF: Altinyayla fault, KF: Kelekci fault, CF: Cameli fault (modified from Yılmaz et al. 2000; Emre et al. 2013)

(McKenzie 1972, 1978; Le Pichon and Angelier 1981; Taymaz et al. 1991; McClusky et al. 2000; Nyst and Thatcher 2004; Catlos et al. 2021 Kalafat et al. 2011; Kadirioğlu et al. 2018; Komut and Karabudak 2021). These tectonic regime and deformation have shaped a large number of fault sets in the region. Normal and oblique faults in the Western Anatolia have caused destructive earthquakes in historical and instrumental periods.

An earthquake with a magnitude of $M_w = 5.6$ (KOERİ 2019) has struck Acipayam, Denizli located in the southwestern part of Anatolia (Fig. 1) on March 20, 2019. The earthquake focal mechanism solutions of KOERİ (2019) and AFAD (2019) demonstrate that it occurred on a NW–SE trending (about N45°–50° E) and NE dipping normal fault with a rake angle of nearly 90°. It has dip–slip normal fault characteristics based on the rake angle. The dip angle is around 45°. More than 1000 aftershocks with magnitudes ranging from 2.0 to 5.1 were recorded and lasted for about 5–6 months. Epicentral distributions of the aftershocks represent an oval-shaped structure with NW direction of the long axis, which proves that movement was on an NW-directed fault. The long axis in the oval shaped aftershock distributions is about approximately 15 km (Fig. 2). In the region, 40 buildings were destroyed and around 400 buildings damaged. The most of those structures are made of mudbrick and have not received any engineering service. The underground water level is too shallow where the damages are very intensive like Yeniköy and Ucari villages. Some small surface cracks have also been observed in the same region.

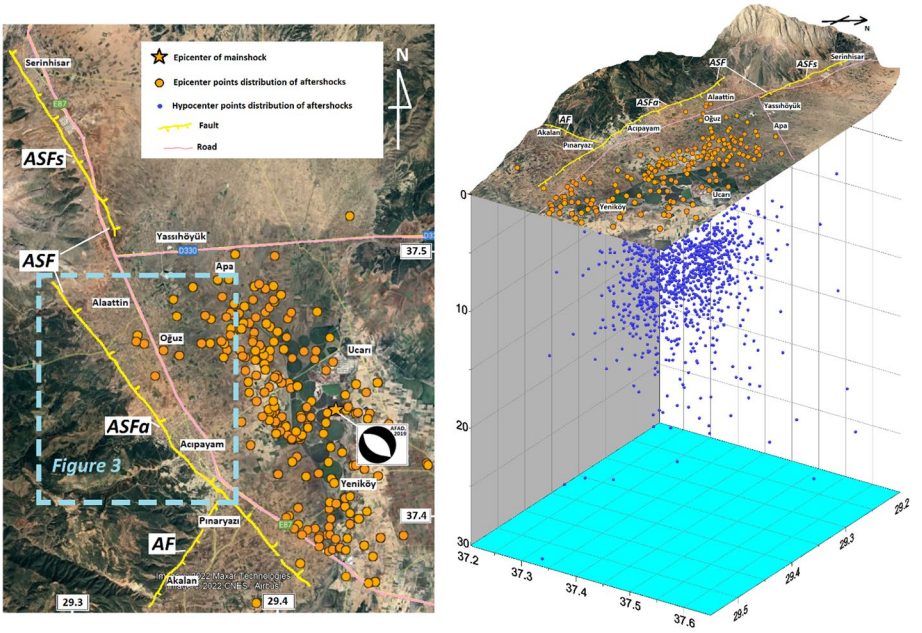

Fig. 2 Epicenters distribution of the Acipayam earthquake aftershocks and focal mechanism solution of the earthquake (http://deprem.afad.gov.tr; http://yerbilimleri.mta.gov.tr; AFAD 2019). Explanations; ASF: Acipayam–Serinhisar fault, ASFa: Acipayam segment of Acipayam–Serinhisar fault, ASFs: Serinhisar segment of Acipayam–Serinhisar fault, AF: Acipayam fault, pink line belong to main road. B: Block diagram belong to hypocenter distribution by depth of the aftershocks

The Acipayam basin extends approximately 4–15 km wide, 40 km long, in the N30° W direction. The basin is in the SE region of the Aegean graben structures, in the NW part of the NE–SW trending Burdur–Fethiye fault zone (Fig. 1). The most important neotectonic structures of the region are the graben–forming normal faults and the Fethiye–Burdur fault zone (Alcicek and ten Veen 2008; Elitez et al. 2016; 2018; Kaymakcı et al. 2018; Özkaptan et al. 2018). The E–W trending graben faults in the west of the Acipayam region are the dominant tectonic structures like Buyuk Menderes graben (BMG), Kucuk Menderes graben (KMG), Gediz–Alasehir graben (GAG), Mugla and Gökova faults. The NW–SE trending grabens (Denizli graben = DG, Dinar graben/half graben and eastern part of the GAG) and NE–SW trending grabens (Civril–Baklan graben = CBG, Acıgöl graben = AG and Burdur graben = BG) are the main tectonic structures (Hancer 2019) as shown in Fig. 1.

The Fethiye–Burdur fault zone is located at the boundary between the eastern region of the South Aegean microplate and the southwest part of the Anatolian microplate (McClusky et al. 2000; Nyst and Thatcher 2004; Catlos et al. 2021). NE-SW trending strike slip dominated the Southwestern Anatolia Shear Zone (SWASZ) is located at the southeast boundary of the Aegean microplate (Çemen et al. 2006; Catlos et al. 2021). This zone is 300 km long and 75–90 km wide and is designated as a left-lateral strike-slip shear zone (Domont et al. 1979; Elitez and Yaltırak 2016). Burdur–Fethiye fault zone is still active (Barka and Reilinger 1997) and moves in left direction between 3 and 4 mm/year in the north and 8–10 mm/year in the south (Elitez et al. 2016). Yagmurlu (2000) emphasized that this zone consists of many fault segments with lengths ranging from 10 to

40 km. Bozcu et al. (2007) refer some faults, which cut the Quaternary sediments, in the Burdur region. The origin of this fault is still controversial. Kaymakcı et al. (2018) propose that there is not a significant strike slip in this zone, and it is usually composed of normal faults. They also state that the Cameli basin in the SW, bounded by normal faults, and the Burdur Basin in the NE are separated from each other by the NW–SE trending right-lateral strike-slip Acipayam transfer zone.

The fault systems between Fethiye and Burdur can be classified into three main groups based on the directions: NE–SW, NW–SE and N–S. In particular, the NE oriented faults limiting Burdur Lake from the north and south have left oblique slip normal fault characteristics. These faults cut the Quaternary formations at many locations. Then, these young units have high slopes and stepped structures that can be observed in the alluvium. The NW trending faults are mostly of normal fault character. They cut the NE trending faults at different locations and caused the development of different segments on these faults (Bozcu et al. 2007).

Acipayam fault (AF), Cameli fault (CF), Kelekçi fault (KF), Altinyayla fault (AyF), which are parallel to each other in the south of Acipayam, and the Burdur fault (BF) located in the NE of this line are shown on the active fault map of Türkiye (Emre et al. 2013). The Cameli and Altinyayla faults are mainly left-lateral strike slip, and the Kelekci fault is dip–slip normal fault on this map (Fig. 1). The Acipayam fault has a normal fault character with a left-lateral strike-slip component. The faults mentioned above have produced many destructive earthquakes both in historical and instrumental periods.

The fault that produced the earthquake on March 20, 2019, is an unknown fault that was not traced and mapped before. However, some researchers performed some studies in the area. Yagmurlu et al. (2017) emphasized that the Acipayam plain is a graben structure, but did not give any information about the formation, age, location and characteristics of the graben and its faults. Kaymakcı et al. (2018) and Özkaptan et al. (2018) implemented some paleomagnetic studies in the region and mentioned the existence of right-lateral strike-slip Acipayam transfer zone that separates the Burdur and the Cameli basins from each other. However, they did not state any fault, forming the transfer zone. Therefore, its existence is unknown until the earthquake on March 20, 2019. It has been documented first time in detail and called the "*Acipayam–Serinhisar fault (ASF)*." This study enlightens the paleoseismological characteristics and the seismic activity of the region by using trench studies in last two millenniums.

2 Geological–tectonical settings of the region

The Anatolian microplate holds the active tectonic structures consist of the North Anatolian Fault (NAF), the East Anatolian Fault (EAF), the Bitlis–Zagros Fold and Thrust Belt (BZTFB), the Dead Sea Fault Zone (DSF), the Cyprus–Hellenic Arc System and the graben systems in the west. The Cyprus–Hellenic Arc System in the west and the Bitlis–Zagros Fold–Thrust Belt in the east are formed the border of African–Arabian and Anatolian Plates (Fig. 1). The northward movement of the African–Arabian Plate at the end of the Middle Miocene creates compressional tectonic regime on the Anatolian Plate and causes westward movement of the Anatolian Plate along the NAF and EAF. The westward movement of the Anatolian microplate turns southwestward in the counterclockwise direction at the west, and thus, the deformation in the western Anatolia still continues (Dewey and Şengör 1979; Le Pichon and Angelier 1979; Domont et al. 1979; Şengör et al.

1985; Meulenkamp et al. 1988; Reilinger et al. 1997; Yılmaz et al. 2000). Various hypotheses have been proposed for the tectonic evolution of the Western Anatolia: (1) the westward escape of the Anatolian Microplate (Dewey and Şengör 1979; Şengör 1979; Şengör et al. 1985), (2) the NE-SW back-arc extension of the Aegean region (McKenzie 1978; Le Pichon and Angelier 1979; Meulenkamp et al. 1988; Yılmaz et al. 2000), (3) the subduction-transform edge propagator fault zone related to the motion of the Hellenic and Cyprus arcs (Govers and Wortel 2005; Hall et al. 2014) and (4) the compressional region of the Western Taurides (Aksu et al. 2009, 2014; Hall et al. 2009, 2014).

The Aegean and south Marmara microplates are located at the west the northwest of the Anatolian microplate, respectively (Nyst and Thatcher 2004). The western Anatolia is positioned at the boundary between the Aegean and Anatolian microplates. This region is transition zone compressional and extensional tectonic regimes. The extension of the Western Anatolia is accepted as a rollback of the Arabian slab along the Hellenic arc (Catlos et al. 2021). The tearing process of the Aegean and Anatolian microplates leads to intermediate-depth seismicity. Hence, the Aegean and Anatolian microplates are seismically active (Şengör and Yılmaz 1981; Okay et al. 1996; Reilinger et al. 1997; Nyst and Thatcher 2004; Meighan et al. 2013; Catlos et al. 2021).

As a result, numerous destructive earthquakes have occurred in Anatolia from past to present (Soysal et al. 1981; Ayhan et al. 1986; Ambraseys and Finkel 1987; Ambraseys and Jackson 1998; Engdahl and Villasenor 2002; Ersoy et al. 2010; Emre and Duman 2011; Royden and Papanikolaou 2011; Yolsal-Çevikbilen et al. 2014; Karasözen et al. 2016). The western part of the North Anatolian fault in the north, the graben systems, Havran-Balıkesir fault zone, Izmir-Balıkesir transfer zone, Usak-Mugla transfer zone, Southwestern Anatolia Shear Zone in the middle and the Fethiye Burdur fault zone in the south (Çemen et al. 2006; Oner et al. 2010; Sözbilir et al. 2011; Gessner et al. 2013; Özkaymak et al. 2013; Uzel et al. 2013; Karaoğlu and Helvacı 2014; Seghedi et al. 2015; Hall et al. 2014) deform Western Anatolia tectonically (Fig. 1). The Acipayam region is located in SW Anatolia and lies between the east of the graben systems and the Fethiye–Burdur fault zone. There are a large number of studies on the active tectonics and seismicity of the region, and geo-tectonical evaluation of it is still controversial. Some researchers (Domont et al. 1979; Şaroğlu et al. 1987; Barka and Reilinger 1997; Elitez and Yaltırak 2016) claim that the Fethiye–Burdur fault zone is left–lateral strike–slip faults, while some others (Koçyiğit 1984; Kaymakcı et al. 2018; Özkaptan et al. 2018; Alcicek and ten Veen 2008) suggest that the relevant zone has normal fault characteristics.

There are a large number of earthquakes in the region between Fethiye and Burdur both in historical and instrumental periods (Fig. 1). The most familiar one in the historical period has destroyed the ancient city of Kibyre at AD 23. In the instrumental period, some of them were Burdur ($M_w = 7.1$) in 1914, Mugla ($M_w = 5.7$ and 6.0) in 1941, Fethiye ($M_w = 7.1$) in 1957, Köycegiz ($= 5.7$) in 1959, Karamanli ($M_w = 5.7$) in 1967, Fethiye ($M_w = 6.2$) in 1969, Burdur ($M_w = 6.2$) in 1971, Gölhisar ($M_w = 5.3$) in 1990 and Cameli ($M_w = 5.1$) in 2007 (Ergin et al. 1967; Soysal et al. 1981; Ambraseys and Finkel 1987; Taymaz and Price 1992; Taymaz et al. 1990; Akyüz and Altunel 2001; Kumsar et al. 2007; Tan et al. 2008; Alcicek 2010; Över et al. 2010). The most of these earthquakes mentioned above are on the Fethiye–Burdur fault zone. The historical earthquake records were found by the paleoseismological studies on the Acipayam fault. Kürçer et al. (2016) detected a seismic event by trench data on the Acipayam fault in Örenköy site (south of Acipayam) at BC 3030–2410. The instrumental records show an earthquake with a magnitude of 5.3 occurred in 1936 (Kumsar et al. 2020). The epicenter of this earthquake corresponds to the north end of the NE–SW trending Acipayam fault. However, there is not clear evidence as

to whether this earthquake was on the Acipayam fault of the Burdur–Fethiye Fault Zone or on the Acipayam–Serinhisar fault.

The NE–SW trending Acipayam fault, close to the studied earthquake, is in a normal fault character with N35° E orientation. It consists of two separate segments and has a total length of 50 km. Radiocarbon dating suggest that it was active in the Holocene (Kürçer et al. 2016). After the Acipayam earthquake it was supposed that it arose on the NE–SW trending Acipayam segment, which is a part of the Fethiye Burdur fault zone, and its epicenter was located in the Acipayam plain. However, the focal mechanism solutions given by KOERI (2019) and AFAD (2019) suggest that a NW–SE trending NE dipping normal fault has produced the earthquake. The distribution of the aftershocks of the earthquake according to their depth illustrates that they are concentrated at an average depth of 10 km (Fig. 2).

Geologically, the rocks of Lycian nappes are seen intensively along a NE–SW trending line extending from Fethiye to Burdur. Lycian nappes, which cross the Menderes Massif with the closure of the northern part of Neotethys along the Izmir–suture zone and move onto the Beydaglari autochthon, consist of ophiolitic rocks, limestone blocks and melange type units. They are observed as various tectonic slices in SW Anatolia, and their settlement ages are post-Lower Miocene (Burdigalian) (Graciansky 1967; Brunn et al. 1970; Ersoy 1990). In the upper part, there are Miocene–Pliocene terrestrial–lacustrine clastic and carbonate sediments (Alcicek and ten Veen 2008; Emre et al. 2013; Elitez et al. 2016; Elitez et al. 2018; Yagmurlu et al. 2017; Kaymakcı et al. 2018). There are Quaternary aged talus deposits and alluvium units at the top.

3 Tectonic and paleoseismological settings of the study area

3.1 Acipayam–Serinhisar Fault (ASF)

The Fethiye–Burdur fault zone is mainly consists of normal faults and shows partially oblique slip (Kaymakcı et al. 2018; Özkaptan et al. 2018; Alcicek and ten Veen 2008). This system extends in NE–SW direction. The Acipayam fault forms the NW end of this zone. ASF is NW–SE trending and is a release fault that develops perpendicular to the Fethiye–Burdur fault zone and therefore to the Acıpayam fault. The ASF is a dip slip normal fault, and its slickenlines and dip slip can be clearly seen on a fault surface at a road cut in south of Acipayam (Fig. 4d). Additionally, the strata inclinations on the hanging wall of the fault support the above data. Synthetic and antithetic fractures shown in Figs. 6 and 7 characterize the tectonic extension. Elitez et al. (2016) state that the Fethiye–Burdur fault zone has a slip rate of 3–4 mm/year in the north and 8–10 mm/year in the south. The Acipayam Serinhisar fault is a small fault with a length of 9 km in the system.

The Acipayam–Serinhisar Fault, which caused the earthquake on March 20, 2019, starts from the south of Acipayam town and extending toward Serinhisar town in the NW, and it has an average N45° W strike, dipping NE with an angle varying between 55° and 65° (Fig. 3). ASF can be divided into the Acipayam segment (ASFa) in the south and the Serinhisar segment (ASFs) in the north (Fig. 2). The length of the ASFa is about 12 km and can be traced up from Acipayam to the NW of Alaattin town. The extension of the fault from that point further to the NW (toward the Serinhisar town) is indistinct. Because in the NW of Alaattin town, where the fault should continue, there is a morphological barrier consisting of a large limestone block. Along this obstacle, the ASF leaps approximately 2.5 km

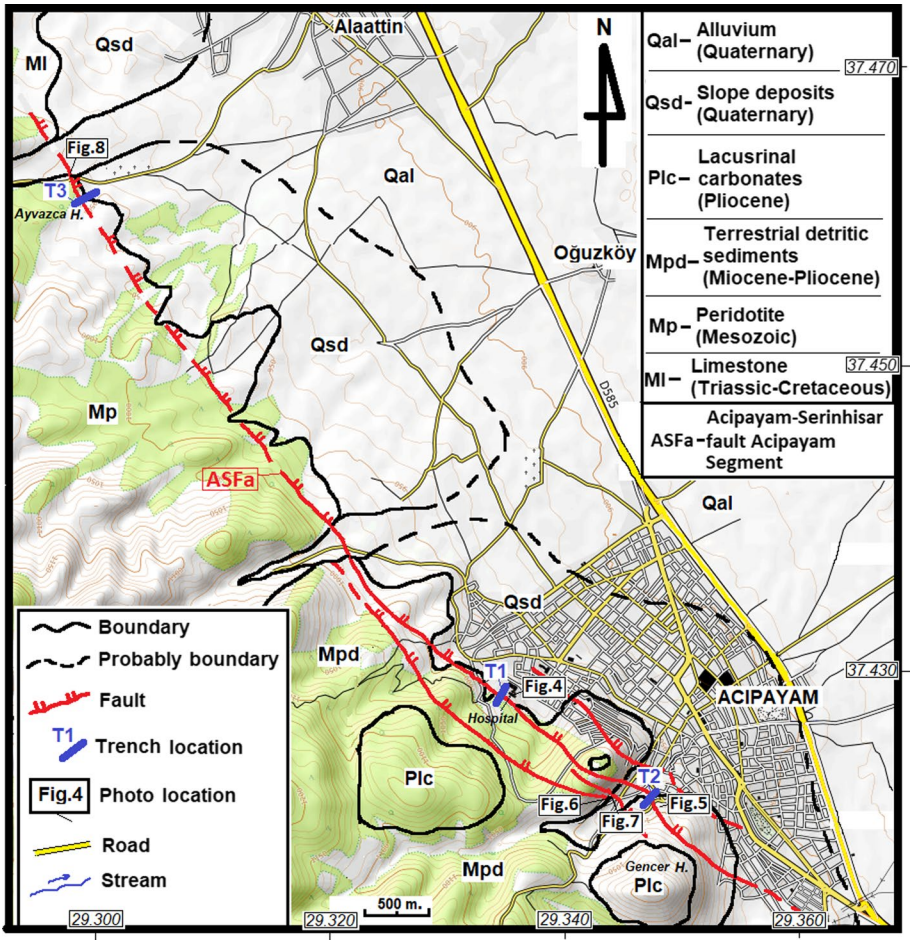

Fig. 3 Geological, tectonial map showing figure and trench locations of the study area and position Acipayam segment (ASFa) of the Acipayam–Serinhisar fault (ASF) (https://opentopomap.org)

NE. This leap is quite evident in the morphotectonic structure of the region. The SW border of the plain continues along a line between Alaattin town and Yassıhöyük suddenly narrows at NE. The Acipayam plain is 12 km wide in the south; it is 6–7 km wide in the northern part. Thus, the continuation of the ASF to the NW remains around Yassıhöyük and ends around Serinhisar (Figs. 2, 4a, b).

There is a morphological lineament between Yassıhüyük and Serinhisar, but there is not any other fault evidence at this 9 km long section. Moreover, the distribution of aftershocks is concentrated in the southern region of Yassıhüyük. They were not recorded between Yassıhüyük and Serinhisar. Therefore, its section between Pinaryazi in the south and Alaattin town in the north has been studied in this paper. The continuation of the fault toward SE has not been detected after Pinaryazi because of the alluvium sediments.

The fault zone is observed as three separate segments parallel to each other at Acipayam town, and the main fault in this zone can be clearly witnessed at the Acipayam State Hospital. Its position at this location is N52° W/85° NE (Fig. 4). The slickenlines of the fault

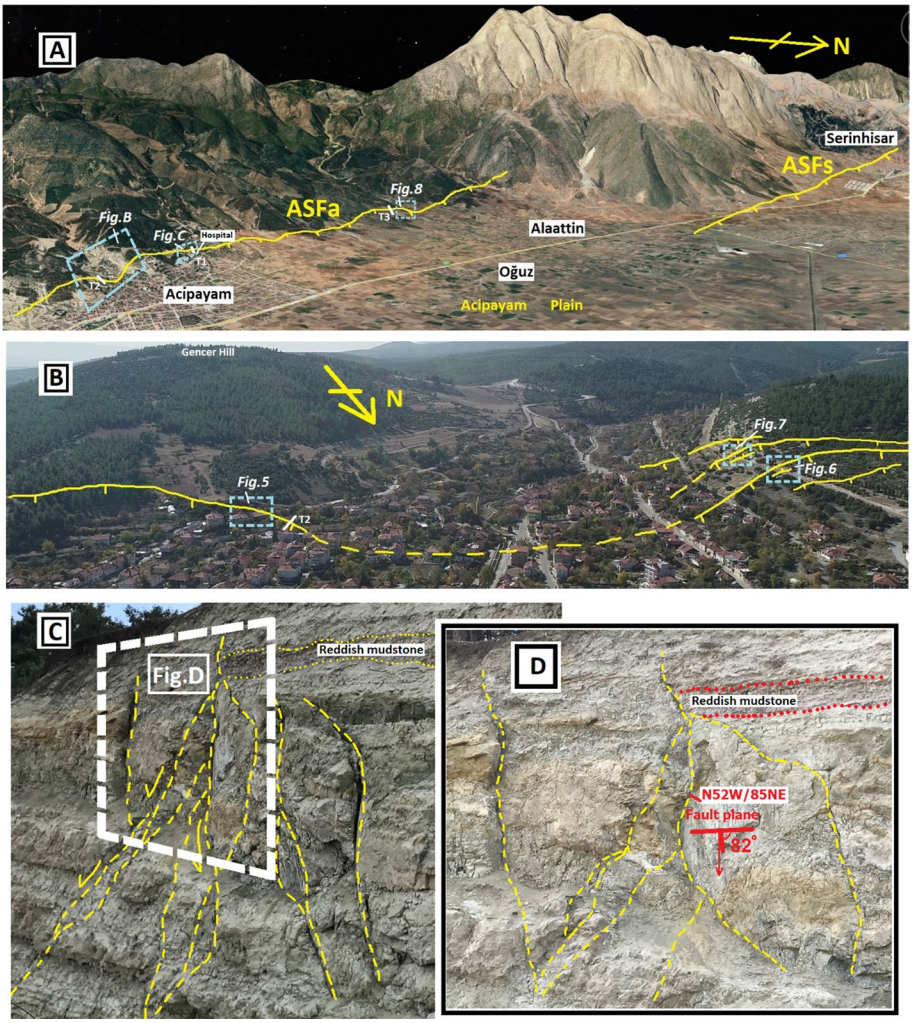

Fig. 4 General view of Acipayam and Serinhisar segments of the ASF on the region (A), location of the fault segment in south of Acipayam (B), general (C) and close (D) images of the Acipayam–Serinhisar fault south of the Acipayam State Hospital (view direction from N to S)

plane, which are in the Miocene terrestrial clastics, indicate some left oblique component. The rake angle on the plane is 82°. At this location, there is a 2–3-m-wide fault zone consisting of small fractures next to the main fault. The same fault was observed at approximately 1 km SE of this point, about 1 km SE and further south with the positions N46° W/70° NE and N44° W/76° NE, respectively (Fig. 5).

There are some synthetic and antithetic fractures developing parallel to this fault just at the south of it. A synthetic fracture was detected 300 m south of the main fault, and its position is N47° W/66° NE. The fault zone, which is seen again in the southern and eastern parts of Acipayam, is a line consisting of many parallel fractures. The positions of the faults are N75° W/85° SW, N50° W/72° NE and N600W/55° NE along the about 10 m long line (Fig. 6). Another fault zone consisting of synthetic and antithetic fractures was observed

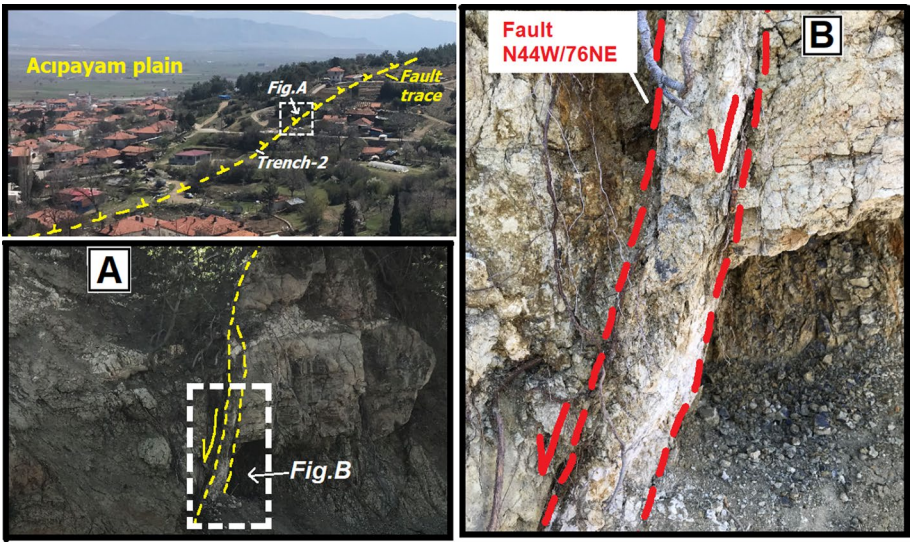

Fig. 5 General image of the Acipayam plain and fault (view direction from W to E) and near images of the fault in the North of the Gencer Hill (A, B) (view direction from NW to SE)

nearly 20 m north of this location, with the positions of N41° W/78° SW, N45° W/70° SW and N52° W/66° NE (Fig. 7). The main fault continues toward NW, and it resurfaced again in the north of Ayvazca Hill, approximately 2 km SW of the Alaattin town. Here, the position of the main fault with a synthetic fracture is N30° W/66° NE (Fig. 8). Yang et al. (2020), using Sentinel 1A interferometric satellite radar images after the earthquake, point out that the earthquake occurred because of normal faulting and that the NE–sloping fault had very little post–directional strike–slip component. They were also expressed that the fault, caused the earthquake, was a blind fault, and there was some increased stress in the NW and SE segments of the fault which could produce earthquakes of $M = 4.8–4.9$.

3.2 Paleoseismological studies

Historical earthquake data are vital for a hazard risk assessment of the region. Some paleoseismological trench studies were carried out at three different locations on the fault line to trace the earthquakes in the past a few millenniums. They were mapped and documented, and the details are given below.

3.2.1 Trench-1 (T1)

The continuation of the ASF fault zone toward the NW was followed, and it was decided to open Trench-1 on the location where the geological–topographic conditions are suitable (Fig. 4c, d). Trench-1, excavated at the west of Acipayam State Hospital, is in the direction of N45° E and is 21 m long, and the study was carried out on the SE wall of it. The coordinates of SW end NE end of the trench are 29.33383619; 37.42816728, and 29.33398103; 37.42835046, respectively. The trench stratigraphy is as follows:

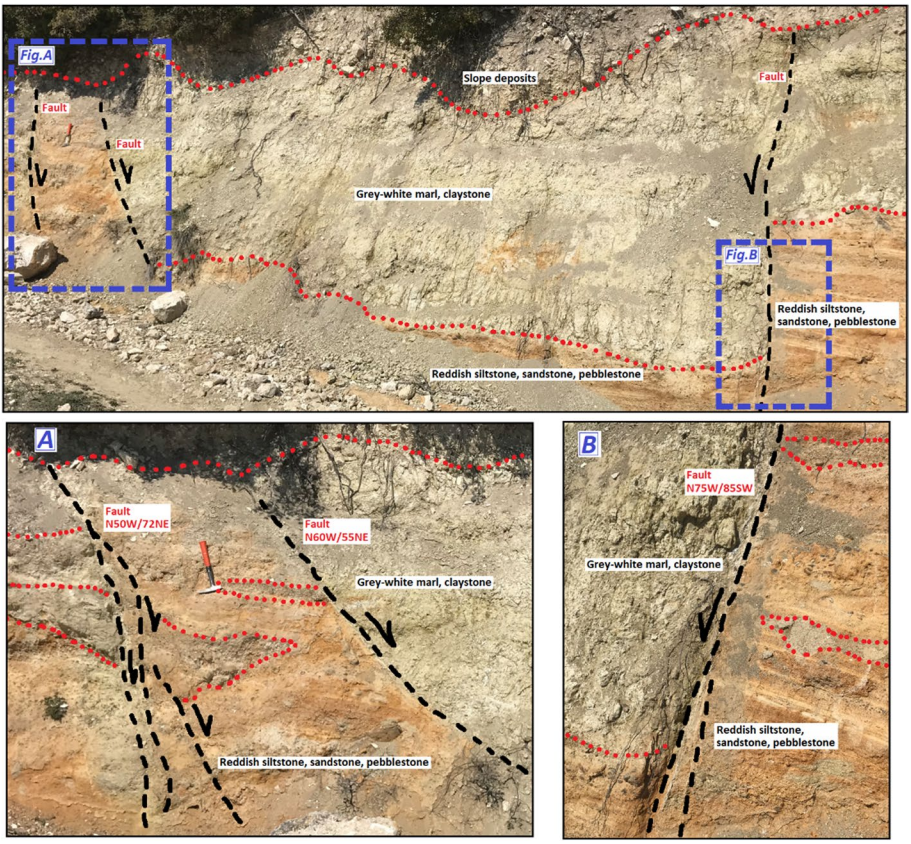

Fig. 6 General and close images (A, B) of the synthetic and antithetic faults in the SW of the Acipayam–Serinhisar fault zone (view direction from SE to NW)

At the bottom, there is gray- and white-colored marl (unit A). The base of the unit cannot be seen, and it is located in the middle and the NE part of the trench. It has 70–80 cm thickness, and it gets thinner up to 10–15 cm at the upper level. In the upper level, there is a dark gray clay (unit B) with a thickness exceeding 2 m. A white–gray–white marl layers (unit C) embedded in unit B as a thin layer. It is seen throughout the entire trench. Over it, toward the NE end of the trench, there is a light gray-colored clay (unit D) reaching up to 2 m thick, as it decreases up to 20 cm toward the SW end of the trench. A thin layer of yellow clay (E unit) lies above this unit. Above it, a light gray-yellow clay (unit F) in 70–80 cm thickness and a brown-yellow clay (G unit) are found at the top. These units are belong to Neogene aged sediments, and they are overlain by a gray clay silt (unit H). It is observed at the NE end of the trench, and its thickness is around 1 m. Stratigraphically, there is young brown clay, sand and gravel (unit I) at the top. Colluvial wedge looking this unit is settled in front of the fault zone. At the top, there is an irregular level of clay, sand and gravel (unit J) covering all units and fault. This unit, whose thickness increases toward the NE edge of the trench, especially after the fault zone, is considered as the second young sedimentary level. An artificial fill (unit K) reaching approximately 3 m is spotted at the far NE end of the trench (Fig. 9).

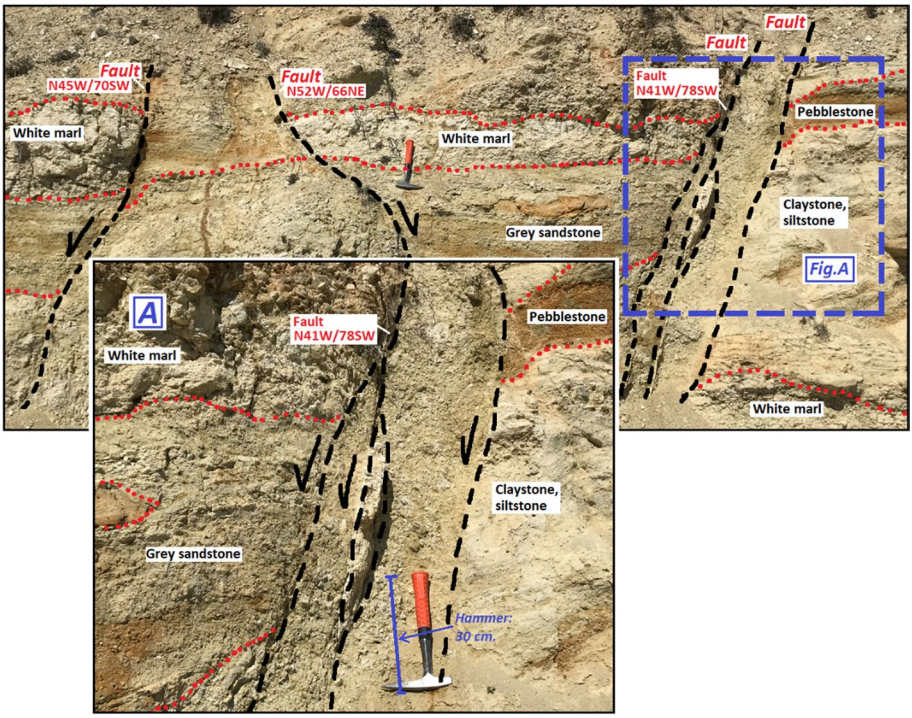

Fig. 7 General and close images (A, B) belong to the synthetic and antithetic faults of the Acipayam–Serinhisar fault zone far from 15 m north of Fig. 6 (view from SE to NW)

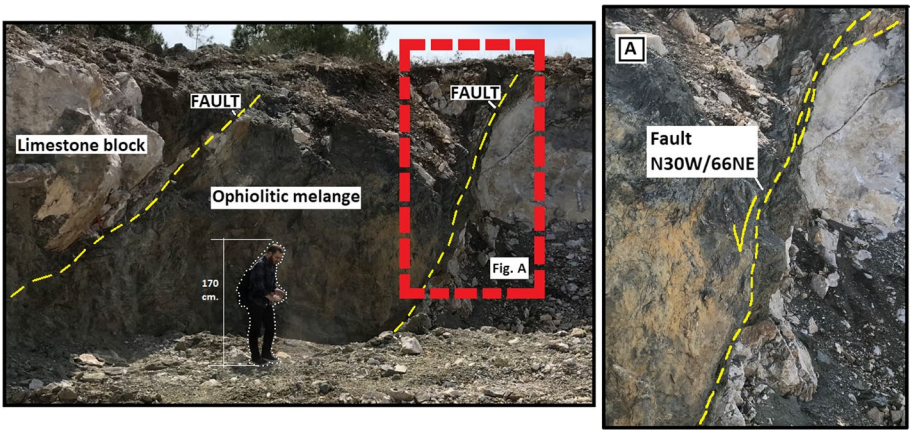

Fig. 8 General and close images of the Acipayam–Serinhisar fault zone in the SW of Alaattin Town (view from NW to SE)

A fault zone has been traced between 10 and 11 m from the NE end of Trench-1 (Fig. 10). The main fault in this zone, which is observed on more than one plane, is a normal fault oriented in N52° W/58° NE direction and has 105 cm total dip slip. The fault

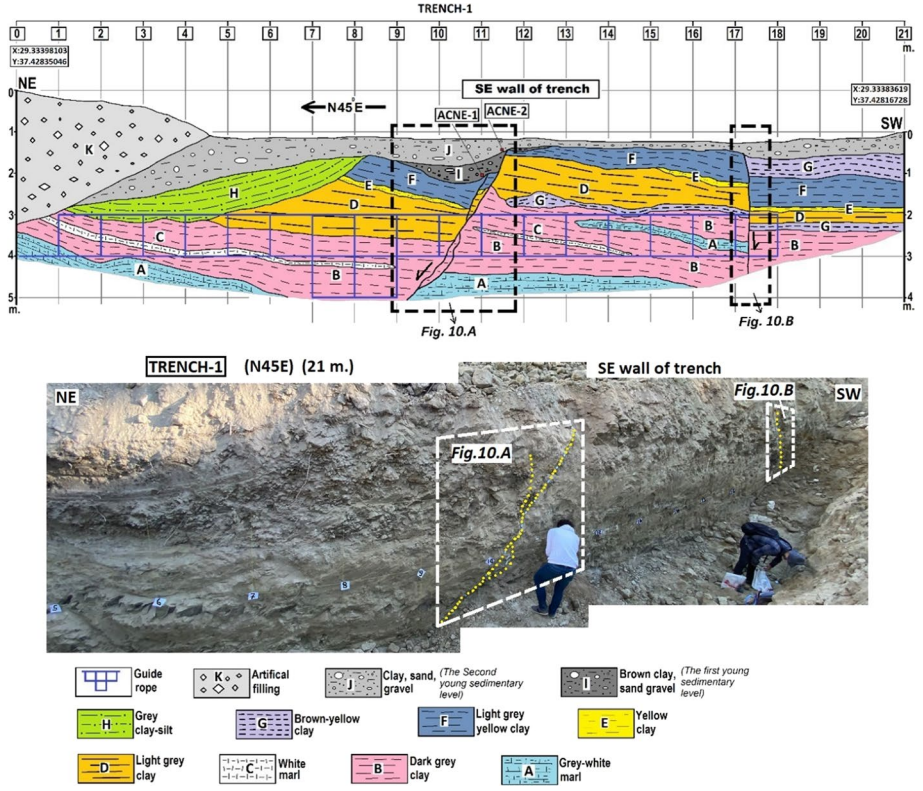

Fig. 9 View of Trench-1 and the geological cross section on the SE wall of the trench (explanations of the geological units and faults are in text)

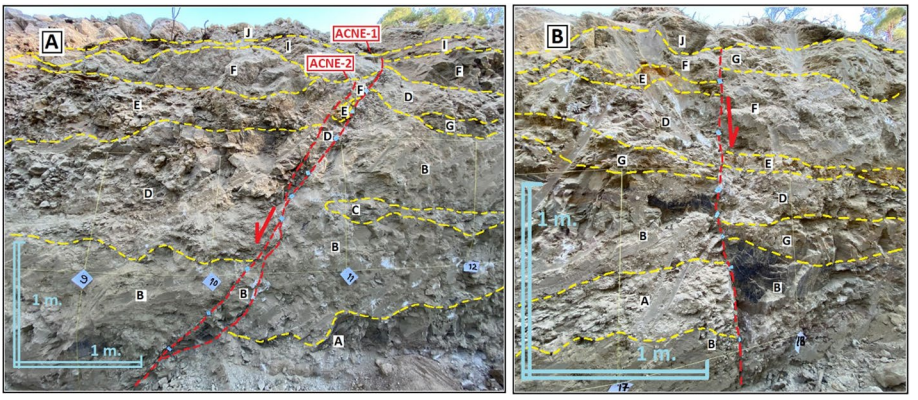

Fig. 10 Detailed views of the cross section between 9 and 12th m (**A**) and 17th and 18th m (**B**) from NE to SW in Trench-1 (fault lines in red, unit boundaries in yellow). (Explanations of units and faults are in text) (see Fig. 9)

zone is covered by two distinct young sedimentary units, namely a mixture of brown clay, sand and gravel, and irregular clay, sand and gravel. The fracture plane, formed just after the first movement, is covered by the first young sedimentary unit (unit I). The obtained field data on the same fracture showed that this unit (unit I) was also cut by the later movement of the same fault plane. The new fracture formed with the later movement of the fault plane is covered by the second young unit (unit J). The offset of the fault in this section is around 55 cm. The data suggest that the fault has relocated in two different periods, and the displacement of the first fracture is around 50 cm. Some samples from the basement levels of these sediments covering the both fault planes were collected for ^{14}C dating. The date of the sample (ACNE-1) taken from the brown clay sand gravel level from the lower sedimentary package is 840 ± 24 years. The calendar age is AD 1168–1263. The ^{14}C age of the sample (ACNE-2) taken from the upper level of this sedimentary overlay is 344 ± 30 years, while the calendar age range is between AD 1471 and 1638.

A N40° W vertical fault was traced around 17 m from the NE edge of the trench. It has 65 cm vertical slip and was assessed as an antithetic fracture that developed approximately parallel to the main fault zone observed far from 10–11 m of the trench.

3.2.2 Trench-2 (T2)

The continuation of the ASF fault zone toward the NW was followed, and it was decided to open Trench-2 on the location where the geological–topographic conditions are convenient (Fig. 5). The SE continuation of the fault, which was identified in the south of the Acipayam State Hospital and in Trench-1, was traced on the northern slope of Gencer Hill, south of Acipayam. The N45° W/70° NE-oriented fault is observed on a road cut. Trench-2 was excavated 40 m away from this point. The 17-m-long SE wall of the trench in the N40° E direction was documented. Trench-2 is about 1.5 km SE of Trench-1. The coordinates of SW end NE end of the trench are 29.34744035; 37.42043078, and 29.34760129; 37.42057563, respectively. The trench stratigraphy is as follows:

There is gray plastic clay (unit A) at the bottom. In the upper part, near the SW end of the trench, there is white sandy clay of about 20–30 cm. It is commonly seen in the SW part of the trench. There is a rarely observed white sandy clay level (B unit) above this unit. At the top, near the SW end of the trench, there is a red gravel (C unit) with a thickness of more than 1 m. The rest of the units on latter is seen throughout the trench. They start with brown silt, clay (unit D) unit in which thin white clayey limestone (unit E) lenses are found with thicknesses of 70–80 cm. In the upper part, there is a light-yellow sand (unit F) level with a thickness of about 20 cm in the SW of the trench. Further above, the gray–yellow clay (unit G) level is observed along the whole trench. Its thickness reaches up to 1 m and nestle 40–50 cm gray light brown lenses (unit H). This unit may reach a height of one meter in some places and include some sand lenses (unit I), particularly on the upper levels. In the upper part, there is a white sandy clay unit (unit J) and they are commonly observed as interbedded layers in other units. A light-yellow clay (K unit) positioned on the above units, and it is seen predominantly in the middle and NE sections of the trench. The unit may reach up to more than one meter in some places and contains thin lenses of clayey limestone and sand. In the upper part of the trench, the dark brown–green layered clay (unit L) is densely located in the NE part, and it includes white sand lenses. The clay, sand and gravel (unit M) may reach up to 60 cm in thickness and cover all those the units and fault. Therefore, it is the critical level in the trench. At the top, there are irregular clay, sand, gravel, block and grounded levels (unit N) (Fig. 11).

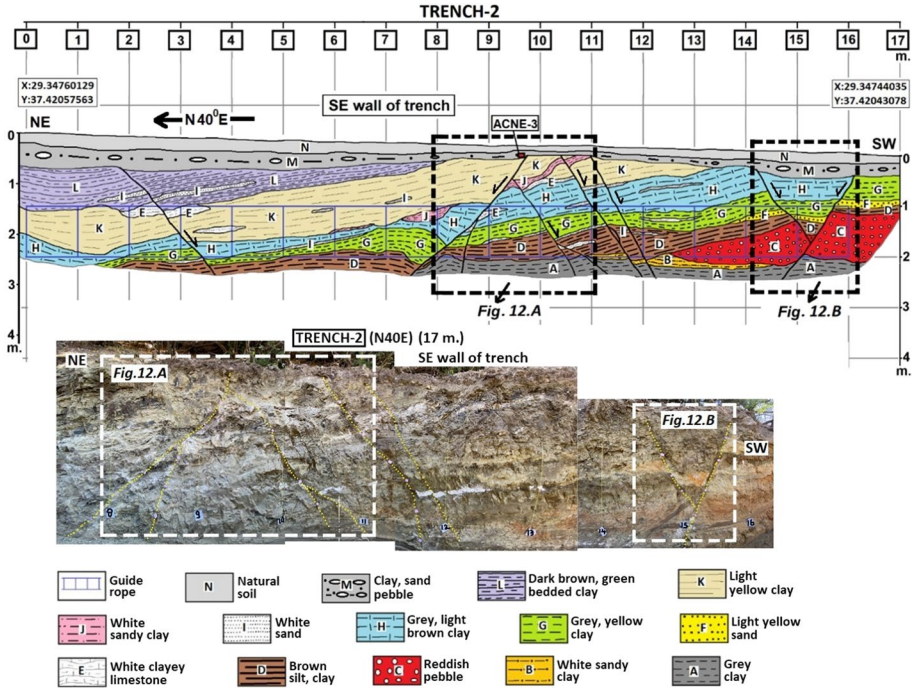

Fig. 11 View of the Trench-2 and the geological cross section on the SE wall of the trench (explanations of the geological units and faults are in text)

A main fault was traced 8–10 m from the NE end of Trench–2. The fault zone reaches about in 7–12 m width with the antithetic faults developed parallel to the main fault (Fig. 12). Here, the position of the fault is N48° W/44° NE, and the dip slip of the fault is around 40 cm. An another antithetic fracture was spotted 2–3 m from the NE of Trench–2 and its offset is around 15 cm. Additionally, two more faults were detected at NE of the

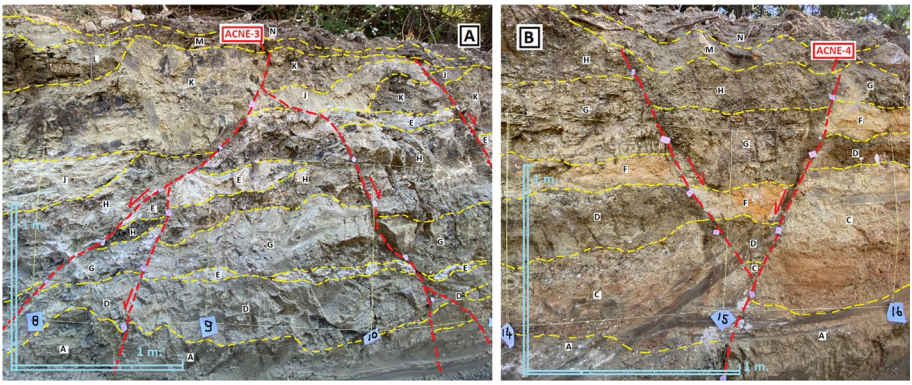

Fig. 12 Detailed views of the cross section between 8 and 11th m (**A**) and, 14th and 16th m (**B**) from NE to SW in Trench-2 (Fault lines in red, unit boundaries in yellow) (explanations of units and faults are in text) (see Fig. 11)

trench. They form a mini graben structure, and the distance between them is 14–16 m. These faults cut the antithetic fault, which is synthetic to the main fault. The offsets of the both faults are around 15–20 cm.

The fault detected between 9 and 10 m from NE of Trench-2 was assessed as the main fault of the trench, and the others as synthetic and antithetic fractures developed parallel to this fault. The ^{14}C dating sample (ACNE-3) taken from the bottom of the sediments overlying the main fault offered 720 ± 36 years of age. The calendar age is AD 1227–1308 or less likely AD 1363–1385.

3.2.3 Trench-3 (T3)

The continuation of the ASF fault zone toward the SW was followed, and it was decided to open Trench-3 on the location where the geological–topographic conditions are convenient (Fig. 8). The fault caused the earthquake was traced toward NW, and a fault zone was observed on the western slope of Ayvazca Hill at the NW of Acipayam (W–SW of the Alaattin town). The Trench–3 was excavated at a convenient location in this region. The trench length is 17 m in N80° E direction, and its NW wall is documented. The coordinates of the trench are at the SW and NE 29.29827546; 37.46178367, and 29.29847395; 37.46181774, respectively. The trench stratigraphy is as follows:

At the bottom, there is weathered serpentinite (unit A) with a thickness exceeding 1 m at the SW end of the trench. Above this, a serpentine (B unit) with a thickness of around 1.0–1.5 m is placed. These units are not observed on the hanging wall of the fault detected in the trench. In the upper part, there is a melange (unit C), mostly composed of ophiolitic origin material. It is located at 1–5 m, 7–9 m and 9–12 m on the hanging wall of the fault and presents an irregular and heavily altered structure. Stratigraphically, a brown clay (unit D) overlies the melange. This unit is found on the hanging wall of the fault with a thickness of more than 2 m. There are clayey gravel (unit E) levels with 15–20 cm thickness embedded in the latter unit. All these units and the fault zone are covered by a unit (unit F), which is a mixture of clay, sand and gravel and it covers the fault. At the top, there is an irregular level of clay, sand, gravel and block (unit G), referred to as natural soil (Fig. 13).

A fault was found at 7–9 m away from the SW end of Trench-3. It is a normal fault in N30° W/42° NE direction (Fig. 14). While there are rock units such as serpentinite in the footwall of the fault, there are sedimentary rocks on the hanging wall. The fault has a total dip slip of 60 cm. A sample was taken for dating from the base level of the young sediment overlying the fault and coded as ACNE-5. Its average age is about 2162 ± 34 years. The results are different in calendar years; BC 235–95 (53.9% probability) and BC 359–276 (36.6% probability). It may unlikely be BC 74–56 and BC 261–244.

4 Summary of paleoseismological observations

Paleoseismological studies were carried out in three trenches on the Acipayam–Serinhisar fault zone and the results evaluated based on the ^{14}C data. A NW–SE trending, NE dipping fault with 60 cm offset in Trench-3 was detected and it covered by clay, sand and gravel (unit F). The dating sample (ACNE-5), taken from the basement level of the sediments covered the fault, has proposed its age as 2162 ± 34 years. As the calendar year, it is at BC 235–95 with 53.9% probability, 359–276 BC with 36.6% probability, BC 74–56 with 2.6% probability and BC 261–244 with 2.4% probability (Table 1). It offers that there was a

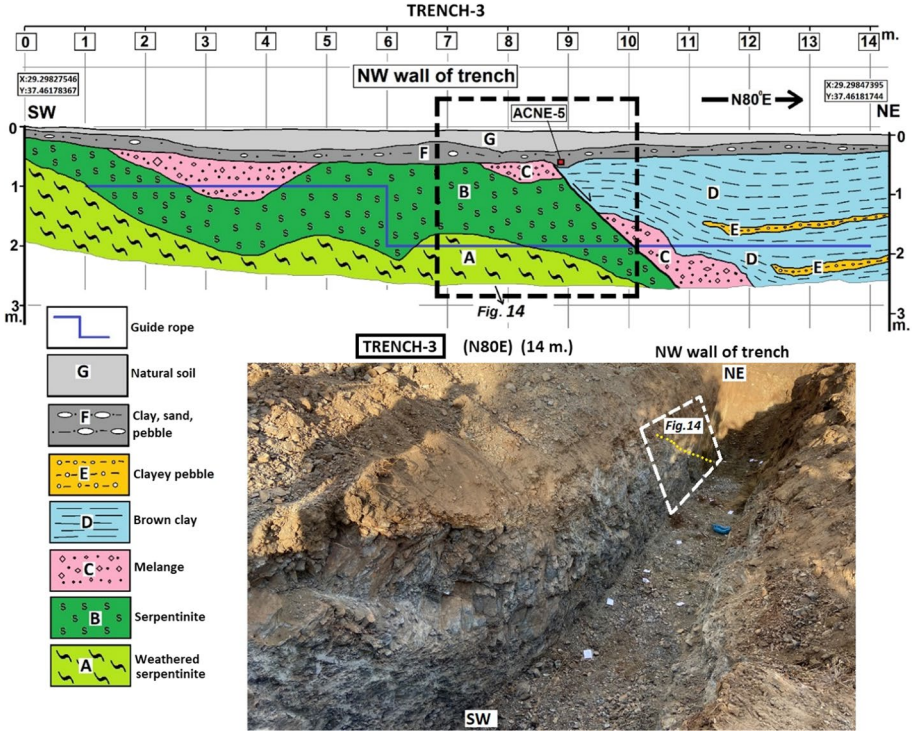

Fig. 13 View of the Trench-3 and the geological cross section on the NW wall of the trench (explanations of the geological units and fault are in text)

Fig. 14 Detailed view of the cross section between 7th and 10th m from SW to NE in Trench-3 (fault lines in red, unit boundaries in yellow) (explanations of units and faults are in text) (see Fig. 13)

Table 1 Results of the radiocarbon date analysis (TUBITAK Marmara Research center) (OxCal v4.4.2 Bronk Ramsey 2009; r.5 Atmospheric data from Reimer et al. 2020)

Trench name	Sample number	Lab. ID number	Material type	Radiocarbon age (BP)	d13C	2 Sigma calibration
Trench-1	ACNE-1	TUBITAK-1522	Sediment	840 ± 24	− 21.7 ± 0.6	1168–1263 (CalAD) (%95.4)
Trench-1	ACNE-2	TUBITAK-1523	Sediment	344 ± 30	− 28.2 ± 1.3	1471–1638 (CalAD) (%95.4)
Trench-2	ACNE-3	TUBITAK-1524	Sediment	720 ± 36	− 26.4 ± 1.6	1227–1308 (CalAD) (%83.1) 1363–1385 (CalAD) (%12.4)
Trench-3	ACNE-5	TUBITAK-1526	Sediment	2162 ± 34	− 24.5 ± 1.3	235–95 (CalBC) (%53.9) 359–276 (CalBC) (%36.6) 74–56 (CalBC) (%2.6) 261–244 (CalBC) (%2.4)

seismic event on the Acipayam–Serinhisar fault zone at BC 235–95. It has caused a 60 cm slip around Alaattin town at the NW part of the fault zone. However, it may be hard to reach the sound comment it is because that only one fault was traced in the trench and the dating range is very wide.

The Trench-2 was opened in the north of Gencer Hill in the SE area of the fault in the Acipayam–Serinhisar fault zone. A fault zone was observed 8–12 m from the NE end of the trench. Additionally, seven faults in various sizes were detected in this zone. The main fault cuts the others and has more slip amount with NW–SE trending and NE dipping. The dating analysis was implemented on the samples (ACNE-3) taken from the bottom of the young sediments overlying the fault. Two more faults resembling a graben structure were observed 14–16 m from the NE of Trench-2, and the fault observed in 16 m was considered as the main fault, because it cuts the other units. The ACNE–3 sample taken from the same trench indicates 720 ± 36 years. This corresponds to the calendar year AD 1227–1385 with 83.1% probability and AD 1363–1385 with 12.4% probability. This designates that there was a seismic event in the range of AD 1227–1385 in the SE part of the fault zone (Fig. 15).

Two fault zones were identified in the Trench-1 opened in the middle of the Acipayam–Serinhisar fault zone. The fault, which was detected around 17 m from the NE end of the trench, is nearly vertical and was appraised as a small fracture plane developed parallel to the main fault. The fault detected 9–12 m from the NE end of the trench is paleoseismologically remarkable. The detailed studies proved that it is the same fault detected in Trench-2. The comprehensive practice in Trench-1 propounds the seismic event of the fault at two different times. It is because the fault zone includes two planes. The first fault plane cuts and offsets the prior sediments by 50 cm. The first plane was cut by the second one and seperated about 55 cm.

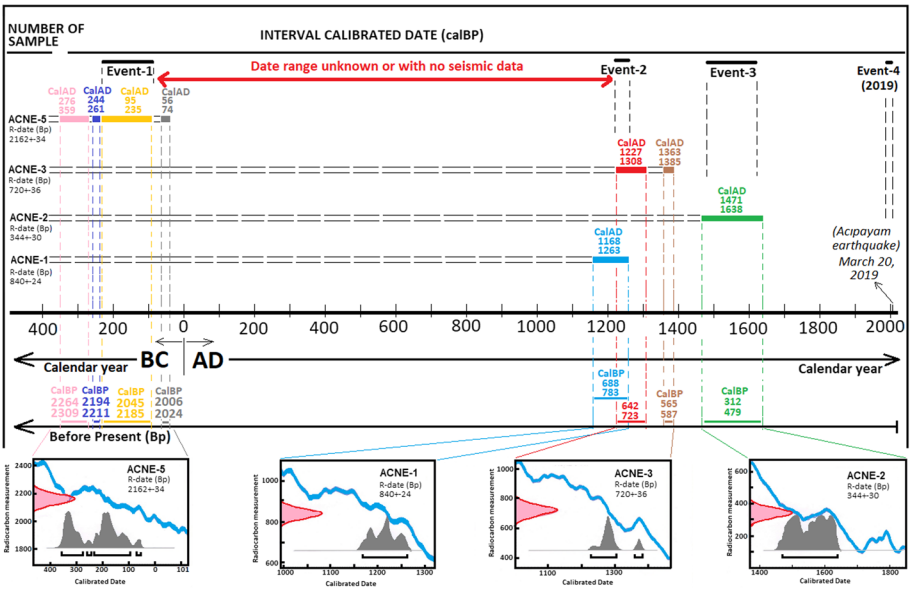

Fig. 15 Distribution chart of probable earthquakes on the Acipayam–Serinhisar fault zone based on radiocarbon dating analysis (calibrated date and radiocarbon date) of the samples collected from Trench-1, 2 and 3. (detailed explanations are given under the "Summary of Paleoseismological Observations" title in text)

One of the young sediments (brown clay, sand, gravel) is covered some part of the fault plane (first fracture plane), and the other part of this level was cut by another plane of the same fault (second fracture plane). This sedimentary level was evaluated as the first young sedimentary unit (unit I) after the fault movement. In the SW of the trench, a small part of the same level was observed on the hanging wall of the fault.

The other sedimentary level (irregular level of clay, sand and gravel) is covered the first fracture plane of the fault and the first young sedimentary unit. This level is called as the second young sedimentary unit (unit J), and it is clearly witnessed that it completely covers the both planes of the fault. Therefore, it is clear enough that the fault zone has moved 50 cm in the first and 55 cm in the second seismic event at this location.

5 Discussion and conclusion

A fault segment, which is a part of NW section of the Acipayam–Serinhisar fault zone, has been detected in Trench-3. It has NW–SE trending, NE dipping with 60 cm offset. The dating of the sample (ACNE-5) taken from the basement level of the sediments overlying the fault indicates a carbon age of 2162 ± 34. As a calendar year, it refers to BC 235–95 with a probability of 53.9%. The obtained data suggest a seismic event on the Acipayam–Serinhisar fault zone in BC 235–95. Thus, an earthquake that caused a 60 cm offset might have occurred around Alaattin town in the NW part of the fault zone. Nevertheless, reaching to the sound results may be difficult due to tracing only one fault in the trench and a very wide range of ^{14}C age.

However, a magnitude 6.5 earthquake may be arisen at the region in the mentioned period and may have caused a 14-km-long surface rupture based on comparison of the observed data to the literature (Schwartz and Coppersmith 1984; Wells and Coppersmith 1994; Pavlides and Caputo 2004). This may be considered as the first seismic event (Event-1) based on the obtained data in the trenches.

The ^{14}C age of the ACNE-1 taken from the bottom level of the first young sedimentary unit in the Trench–1 is 840 ± 24, and its calendar age is AD 1168–1263. The date of ACNE-3, which is on the same fault and detected in the Trench-2, shows the calendar year AD 1227–1308. This finding proposes that the fault may have produced an earthquake that created a surface rupture in these years, especially at AD 1227–1263. The damage and death rate may be ignored because of the low population of Acipayam and nearby 750–800 years ago. The first seismic event has generated 50 cm slip in Trench-1 and 40 cm slip in Trench-2. Considering that a fault creates a maximum slip of 50 cm, it corresponds to an earthquake $M_w = 6.3$–6.4 according to the earthquake–fault empirical relations mentioned above. The probable surface rupture length in the earthquake should be around 10 km according to the literature (Schwartz and Coppersmith 1984; Wells and Coppersmith 1994; Pavlides and Caputo 2004). This activity was called as the second seismic event (Event-2) based on the data obtained from the trenches.

A second seismic event may have occurred in Trench-1 after the first one. The dating sample (ACNE-2), which was taken at the base level that cut the first young sedimentary unit and re-cut the second younger sedimentary unit overlying the fault, points out 344 ± 30 years and the calendar age of the AD 1471–1638. It verifies that the fault has broken and moved 55 cm at AD 1471–1638 for the second time. Such an earthquake has not declared in the historical records. This seismic event probably corresponds to a magnitude 6.3–6.4 earthquake and about 10 km surface rupture (Schwartz and Coppersmith 1984;

Wells and Coppersmith 1994; Pavlides and Caputo 2004). This case suggests the third seismic event (Event-3). The March 20, 2019, a magnitude of 5.6 earthquake was considered as the fourth seismic event (Event-4) in this fault zone. Apart from the mentioned events, the earthquakes with deep hypocenters and without any surface rupture may have occurred in the same fault zone. In this case, detecting these earthquakes is not possible because of untracable deformation structures on or near the surface. Although the studied earthquake was effective and destructive, it has not caused any surface rupture. Therefore, any surface deformation has not occur after this earthquake with a 10.7 km hypocenter.

As a result, the Acipayam–Serinhisar fault may have produced earthquakes with surface ruptures three times at BC 100–200, AD 1200s and AD 1500–1600. Considering the last two earthquakes detected in the same trench and on the same fracture, it can be supposed that the fault has broken twice at the same place with an interval of 350 years. However, the 350-year recurrence period suggested by evaluating the age data of only these two seismic events detected in the same trench may not be a proper approach. More data are needed to suggest an appropriate recurrence period because of a long time interval between Event-1 and Event-2. However, the structure of the fault and the deformation structures in underground are not regular and uniform. Moreover, the hypocenter and the magnitude of the earthquake, like the one in 2019, may not create fractures on earth and more earthquakes might be occurred outside of these dates. The historical records reference an earthquake of 5.3 magnitude in the region in 1936 (Kumsar et al. 2020). Although the epicenter of this earthquake appears in the middle of the basin, it also corresponds to the Acipayam fault in the south. Therefore, there is not any evidence about the source fault of this earthquake, and the epicenter location is very likely inaccurate.

The recorded and unrecorded earthquakes (like $M_w = 6.3–6.4$) happened in the past might not be reported in historical literature because of limited destructions and/or long distances to crowded towns. As a result, a fault, not shown on the Active Fault Map of Türkiye, has been mapped and documented in the lights of the field studies and paleoseismic data. Unearthing the unknown faults, updating the active fault map and illuminating the seismic history of these faults are essential for the seismicity and hazard evaluation of the region.

Acknowledgements This study was funded by Pamukkale University BAP (Grant Number 2020FEBE014). The authors also thank to Turhan Dogan of TUBITAK MAM for 14C dating and Dr. Hulusi Sevkan, Mayor of Acipayam, for trench excavations.

Author contributions All authors contributed to study conception and design. Field working and data collection were performed by Mete Hancer and Nebil Kenanoglu. The draft of the manuscript was written by Mete Hancer and Erdal Akyol and all authors commented on previous version of the manuscript. All authors read and approved the final version of it.

Funding This work was supported by Pamukkale University BAP (Grant Number 2020FEBE014).

Declarations

Conflict of interest The authors declare that they have no conflict of interest.

References

AFAD (2019) Preliminary report on 20 Mart 2019 Acipayam (Denizli) Mw5.5 eartquake. T.C. İcisleri Bakanligi, Afet ve Acil Durum Yön., Deprem Dairesi Baskanligi, 10 s. (https://deprem.afad.gov.tr/downloadDocument?id=1667) (in Turkish).

Aksu AE, Hall J, Yaltırak C (2009) Miocene-recent evolution of Anaximander Mountains and finike basin at the junction of Hellenic and Cyprus Arcs, eastern Mediterranean. Mar Geol 258:24–47
Aksu AE, Hall J, Yaltırak C, Çınar E, Küçük M, Çifçi G (2014) Late Miocene–recent evolution of the Finike Basin and its linkages with the Beydağlari complex and the Anaximander Mountains, eastern Mediterranean. Tectonophysics 635:59–79
Akyüz HS, Altunel E (2001) Geological and archaeological evidence for post-Roman earthquake surface faulting at Cibyra, SW Turkey. Geodin Acta 14:95–101
Alcicek H (2010) Stratigraphic correlation of the Neogene basins in southwestern Anatolia: regional palaeogeographical, palaeoclimatic and tectonic implications. Palaeogeogr Palaeoclimatol Palaeoecol 291:297–318
Alcicek MC, ten Veen JH (2008) The late Early Miocene Acipayam piggy-back basin: refining the last stages of Lycian nappe emplacement in SW Turkey. Sediment Geol 208:101–113
Ambraseys NN, Finkel CF (1987) Seismicity of Turkey and neighbouring regions 1899–1915. Annules Geophys 5B:701–726
Ambraseys NN, Jackson JA (1998) Faulting associated with historical and recent earthquakes in the Eastern Mediterranean region. Geophys J Int 133(2):390–406
Ayhan E, Elsan E, Sancaklı N, Er SB (1986) Earthquake catalog of Turkey and surroundings 1881–1980. Boğaziçi Üniv., Kandilli Observatory and Earthquake Research Institute, Istanbul, p 126
Barka A, Reilinger R (1997) Active tectonics of the Eastern Mediterranean region: deduced from GPS, neotectonic and seismicity data. Ann Geophys 40(3):587–610
Bozcu M, Yağmurlu F, Şentürk M (2007) Fethiye−Burdur Fay Zonunun bazı neotektonik ve paleosismolojik özellikleri, GB Türkiye. Jeol Mühendisliği Derg 31(1):25–48 (**in Turkish**)
Bronk Ramsey C (2009) Bayesian analysis of radiocarbon dates. Radiocarbon 51(1):337–360
Brunn JH, Graciansky PC, Gutnic M, Juteau T, Lefevre R, Marcoux J, Monod O, Poisson A (1970) Structures majeures at correlations stratigraphiques dans les Taurides occidentales. B Soc Geol Fr 3:515–556 (**in French**)
Catlos EJ, Etzel TM, Çemen I (2021) Extensional tectonics in Western Anatolia. Eastward continuation of the Aegean extension. AGU Books, Kayseri. https://doi.org/10.1002/essoar.10508671.1
Çemen I, Catlos EJ, Gogus O, Ozerdem C (2006) Postcollisional extensional tectonics and exhumation of the Menderes Massif in the western Anatolia extended terrane, Turkey. Spec Pap Geol Soc Am 409:353–379
Cinti FR, Pantosti D, Lombardi AM, Civico R (2021) Modeling of earthquake chronology from paleoseismic data: insights for regional earthquake recurrence and earthquake storms in the Central Apennines. Tectonophysics 816:229016
Dewey JF, Şengör AMC (1979) Aegean and surrounding regions: complex multiplate and continuum tectonics in a convergent zone. Geol Soc Am Bull 90(1):84–92. https://doi.org/10.1130/0016-7606(1979)902.0.CO;2
Domont JF, Uysal Ş, Şimşek Ş, Karamanderesi IH, Leteouzey J (1979) Formations of grabens in Southwestern Anatolia. Bull Min Res Explor Inst Turk 92:7–18
Elitez I, Yaltırak C (2016) Miocene to quaternary tectonostratigraphic evolution of the middle section of the Burdur−Fethiye Shear Zone, south−western Turkey: implications for the wide inter-plate shear zones. Tectonophysics 690:336–354
Elitez I, Yaltırak C, Aktuğ B (2016) Extensional and compressional regime driven left-lateral shear in southwestern Anatolia (eastern Mediterranean): the Burdur–Fethiye Shear Zone. Tectonophysics 688:26–35
Elitez I, Yaltırak C, Sunal G (2018) A new chronostratigraphy (40Ar−39Ar and U−Pb dating) for the middle section of the Burdur−Fethiye Shear Zone, SW Turkey (eastern Mediterranean). Turk J Earth Sci 27:405–420
Emre Ö, Duman T (2011) Simav-Kutahya earthquake (Mw:5.8) in Turkey pre-assessment, earthquake report. General Directorate of Mineral Research and Exploration (MTA). Earth Dynamics Research Center, Ankara (**in Turkish**)
Emre Ö, Duman TY, Özalp S, Elmacı H, Olgun Ş, Şaroğlu F (2013) Active fault map of Turkiye in 1/1.250.000 scale. Maden Tetkik ve Arama Genel Müdürlüğü Özel Yayınlar Serisi−30, Ankara−Türkiye (in Turkish)
Engdahl ER, Villasenor A (2002) Global seismicity: 1900–1999. In: Lee WHK et al (eds) International handbook of earthquake and engineering seismology, Part A. Academic, San Diego, pp 665–690
Ergin K, Güçlü U, Uz Z (1967) A catalogue of earthquakes for Turkey and surrounding area 11 AD to 1964 AD. ITU Earth Physics Institute Publications, Istanbul
Ersoy Ş (1990) The analysis of evolution and structural items of the western Taurus−Lycian nappes. Bull Chamb Geol Eng Turk 37:5–16 ((**in Turkish**))

Ersoy EY, Helvacı C, Sozbilir H (2010) Tectono-stratigraphic evolution of the NE–SW-trending superimposed Selendi basin: implications for late Cenozoic crustal extension in Western Anatolia, Turkey. Tectonophysics 488:210–232

Gessner K, Gallardo LA, Markwitz V, Ring U, Thomson SN (2013) What caused the denudation of the Menderes Massif; review of crustal evolution, lithosphere structure, and dynamic topography in southwest Turkey. Gondwana Res 24(1):243–274

Govers R, Wortel MJR (2005) Lithosphere tearing at STEP faults: response to edges of subduction zones. Earth Planet Sci Lett 236(1–2):505–523. https://doi.org/10.1016/j.epsl.2005.03.022

Graciansky PC (1967) Existence d'une nappe ophiolitique á l'extrémité occidentale de la chaîne sudanatolienne; relations avec les autres unités charriées et avec les terrains autochtones (Province de MuÂla, Turquie) C. R. Ac. Sc., t., 264, série D, s: 2876−2879 (in French)

Gürboğa Ş, Gökçe O (2019) Paleoseismological catalog of pre-2012 trench studies on the active faults in Turkey. Bull Miner Res Explor 159:63–87. https://doi.org/10.19111/bulletinofmre.561925

Hall J, Aksu AE, Yaltırak C, Winsor JD (2009) Structural architecture of the Rhodes Basin: a deep depocentre that evolved since the Pliocene at the junction of Hellenic and Cyprus Arcs, eastern Mediterranean. Mar Geol 258(1–4):1–23. https://doi.org/10.1016/j.margeo.2008.02.007

Hall J, Aksu AE, Elitez I, Yaltırak C, Çifçi G (2014) The Fethiye-Burdur Fault Zone: a component of upper plate extension of the subduction transform edge propagator fault linking Hellenic and Cyprus Arcs, Eastern Mediterranean. Tectonophysics 635:80–99. https://doi.org/10.1016/j.tecto.2014.05.002

Hancer M (2019) Geological evidences belonging to late Holocene seismic activity in South of Denizli Graben (Southwestern of Turkey, South-East European Part). Carpath J Earth Env Sci 14(1):137–153

Kadirioğlu FT, Kartal RF, Kılıç T, Kalafat D, Duman TY, Eroğlu Azak T, Özalp S, Emre Ö (2018) An improved earthquake catalogue (M ≥ 4.0) for Turkey and its near vicinity (1900–2012). Bull Earthq Eng 16:3317–3338

Kalafat D, Güneş Y, Kekovalı K, Kara M, Deniz P, Yılmazer M (2011) Bütünleştirilmiş Homojen Türkiye Deprem Kataloğu (1900–2010; M ≥ 4.0). Bogazici Üniversitesi, Kandilli Rasathanesi ve Deprem Araştırma Enstitüsü, Yayın No: 1049, 640p. Bebek-İstanbul (in Turkish)

Karaoğlu Ö, Helvacı C (2014) Isotopic evidence for a transition from subduction to slab-tear related volcanism in western Anatolia, Turkey. Lithos 192–195:226–239. https://doi.org/10.1016/j.lithos.2014.02.006

Karasözen E, Nissen E, Bergman EA, Johnson KL, Walters RJ (2016) Normal faulting in the Simav graben of western Turkey reassessed with calibrated earthquake relocations. J Geophys Res Solid Earth 121:4553–4574. https://doi.org/10.1002/2016JB012828

Kaymakcı N, Langereis C, Özkaptan M, Özacar AA, Gülyüz E, Uzel B, Sözbilir H (2018) Paleomagnetic evidence for upper plate response to a Step fault, SW Anatolia. Earth Planet Sci Lett 498:101–115

Koçyiğit A (1984) Intra-plate neotectonic development in Southwestern Turkey and adjacent areas. Bull Geol Soc Turk 27:1–16

KOERİ (2019) Yeniköy−Acipayam−Denizli Depremi Basın Bülteni, B.Ü., Kandilli Rasathanesi ve Deprem Araştırma Enstitüsü, 7 s. (http://www.koeri.boun.edu.tr/sismo/2/wp-content/uploads/2019/03/20_03_2019_ACIPAYAM1.pdf) (in Turkish)

Komut T, Karabudak E (2021) Paleo-earthquake evidence and earthquake recurrence for Düzce fault, Turkey. J Seismol 25:803–823

Kumsar H, Özkul M, İnel M, Hançer M, Tama YS, Ozmen HB et al (2007) Çameli earthquake pre-examination report. Pamukkale University, Denizli, p 55 (**in Turkish**)

Kumsar H, Özkul M, Semiz B (2020) Geotechnical site investigation and evaluation of 20 March 2019 Mw 5.5 Acipayam (Denizli) earthquake. Pajes 26(8):1343–1352

Kürçer A, Özdemir E, Uygun Güldoğan C, Duman TY (2016) The first Paleoseismic trench data from Acipayam fault, Fethiye Burdur fault zone SW Turkey. Bull Geol Soc Greece 50(1):75–84

Le Pichon X, Angelier J (1979) The Hellenic arc and trench system; a key to the neotectonic evolution of the eastern Mediterranean area. Tectonophysics 60:1–42

Le Pichon X, Angelier J (1981) The Aegean Sea. Philos Trans R Soc Lond Ser A Math Phys Sci 300:357–372. https://doi.org/10.1098/rsta.1981.0069

McClusky S, Balassanian S, Barka A, Demir C, Ergintav S, Georgiev I, Gurkan O, Hamburger M, Hurst K, Kahle H, Kastens K, Kekelidze G, King R, Kotzev V, Lenk O, Mahmoud S, Mishin A, Nadariya M, Ouzounis A, Paradissis D, Peter Y, Prilepin M, Reilinger R, Sanli I, Seeger H, Tealeb A, Toksöz MN, Veis G (2000) Global positioning system constraints on plate kinematics and dynamics in the eastern Mediterranean and Caucasus. J Geophys Res 105(B3):5695–5719. https://doi.org/10.1029/1999JB900351

McKenzie D (1972) Active tectonics of the Mediterranean Region. Geophys J R Astron Soc 30:109–185. https://doi.org/10.1111/j.1365-246X.1972.tb02351.x

McKenzie D (1978) Active tectonics of the Alpine-Himalayan belt: the Aegean Sea and surrounding regions. Geophys J R Astron Soc 55:217–254
Meighan HE, ten Brink U, Pulliam J (2013) Slab tears and intermediate-depth seismicity. Geophys Res Lett 40:4244–4248. https://doi.org/10.1002/grl.50830
Meulenkamp JE, Wortel MJR, van Wamel WA, Spakman W, Hoogerduyn SE (1988) On the Hellenic subduction zone and the geodynamic evolution of Crete since the late middle Miocene. Tectonophysics 146:203–215
Nyst M, Thatcher W (2004) New constraints on the active tectonic deformation of the Aegean. J Geophys Res 109(11):23. https://doi.org/10.1029/2003JB002830
Okay AI, Satır M, Maluski H, Siyako M, Monie P, Metzger R, Akyüz S (1996) Paleo- and Neo-Tethyan events in northwestern Turkey: geologic and geochronologic constraints. In: Harrison TM (ed) The tectonic evolution of Asia. Cambridge University Press, Cambridge, pp 420–441
Oner Z, Dilek Y, Kadioglu YK (2010) Geology and geochemistry of the synextensional Salihli granitoid in the Menderes core complex, western Anatolia, Turkey. Int Geol Rev 52(2–3):336–368. https://doi.org/10.1080/00206810902815871
Över S, Pınar A, Özden S, Yılmaz H, Ünlügenç UC, Kamacı Z (2010) Late Cenozoic stress field in the Cameli Basin, SW Turkey. Tectonophysics 492(1):60–72
Özkaptan M, Kaymakci N, Langereis CG, Gülyüz E, Özacar AA, Uzel B, Sözbilir H (2018) Age and kinematics of the Burdur Basin: inferences for the existence of the Fethiye Burdur Fault Zone in SW Anatolia (Turkey). Tectonophysics 744:256–274
Özkaymak C, Sözbilir H, Uzel B (2013) Neogene-quaternary evolution of the Manisa Basin: evidence for variation in the stress pattern of the Izmir-Balikesir Transfer Zone, western Anatolia. J Geodyn 65:117–135
Pavlides S, Caputo R (2004) Magnitude versus faults'surface parameters: quantitative relationships from the Aegean Region. Tectonophysics 380:159–188
Reilinger RE, McClusky SC, Oral MB, King RW, Toksoz MN, Barka AA, Kinik I, Lenk O, Sanli I (1997) Global Positioning System measurements of present-day crustal movements in the Arabia–Africa–Eurasia plate collision zone. J Geophys Res 102(B5):9983–9999. https://doi.org/10.1029/96JB03736
Reimer PJ, Austin WEN, Bard E, Bayliss A, Blackwell PG et al (2020) The IntCal20 northern hemisphere radiocarbon age calibration curve (0–55 cal kBP). Radiocarbon 62(4):1–33
Royden LH, Papanikolaou DJ (2011) Slab segmentation and late Cenozoic disruption of the Hellenic arc. Geochem Geophys Geosyst AGU Geochem Soc. https://doi.org/10.1029/2010GC003280
Şaroğlu F, Emre Ö, Boray A (1987) Active faults of Turkiye and their seismicity. MTA Genel Müdürlüğü, Rapor 8174: 394, Ankara Turkey (in Turkish)
Schwartz PD, Coppersmith KJ (1984) Fault behaviour and characteristic earthquakes: examples from the Wasatch and San Andreas Fault. J Geophys Res 89:5681–5698
Seghedi I, Helvacı C, Pécskay Z (2015) Composite volcanoes in the south-eastern part of İzmir-Balıkesir Transfer Zone, Western Anatolia, Turkey. J Volcanol Geoth Res 291:72–85. https://doi.org/10.1016/j.jvolgeores.2014.12.019
Şengör AMC (1979) The North Anatolian transform fault: its age, offset and tectonic significance. Geol Soc Sp 136:269–282
Şengör AMC, Yılmaz Y (1981) Tethyan evolution of Turkey: a plate tectonic approach. Tectonophysics 75:181–241
Şengör AMC, Görür N, Şaroğlu F (1985) Strike-slip faulting and related basin formation in zones of tectonic escape: Turkey as a case study. In: Biddle KT, Christie-Blick N (eds) Strike-slip faulting and basin formation, Society for Economic Paleontology Mineralogy Special Publications, vol 37, pp 227–264
Soysal H, Sipahioğlu S, Kolçak D, Altınok Y (1981) Historical earthquake catalog of Turkiye and vicinity. TÜBİTAK Proj TBAG 341:85 ((**in Turkish**))
Sözbilir H, Sari B, Uzel B, Sümer Ö, Akkiraz S (2011) Tectonic implications of transtensional supradetachment basin development in an extension-parallel transfer zone: the Kocacay Basin, western Anatolia, Turkey. Basin Res 23:423–448. https://doi.org/10.1111/j.1365-2117.2010.00496.x
Tan O, Tapırdamaz MC, Yörük A (2008) The earthquake catalogues for Turkey. Turk J Earth Sci 17:405–418
Taymaz T, Price S (1992) The 1971 May 12 Burdur earthquake sequence, SW Turkey: a synthesis of seismological and geological observations. Geophys J Int 108:589–603
Taymaz T, Jackson JA, Westaway R (1990) Earthquake mechanisms in the Hellenic Trench near Crete. Geophys J Int 102:695–731
Taymaz T, Jackson J, McKenzie D (1991) Active tectonics of the north and central Aegean Sea. Geophys J Int 106(2):433–490

Uzel B, Sözbilir H, Özkaymak Ç, Kaymakcı N, Langereis CG (2013) Structural evidence for strike-slip deformation in the Izmir-Balıkesir transfer zone and consequences for late Cenozoic evolution of western Anatolia (Turkey). J Geodyn 65:94–116

Wells DL, Coppersmith KJ (1994) New empirical relationships among magnitude, rupture length, rupture width, rupture area, and surface displacement. Bull Seism Soc Am 84(4):974–1002

Yagmurlu F (2000) Seimotectonic features of Burdur Fault. Batı Anadolu'nun depremselligi sempozyumu. Bildiriler, pp 143–152 (in Turkish)

Yagmurlu F, Tagliasacchı E, Şentürk M (2017) The role of ophiolitic rocks to form heavy mineral plasters: Burdur Camköy case: SW Turkiye. Yerbilimleri 38(3):259–274 (**in Turkish**)

Yang J, Xu C, Wang S, Wang X (2020) Sentinel-1 observation of 2019 Mw 5.7 Acipayam earthquake: A blind normal-faulting event in the Acipayam basin, southwestern Turkey. J Geodyn 135:101707

Yılmaz Y, Genç SC, Gürer OF, Bozcu M, Yılmaz K, Karacık Z, Altunkaynak Ş, Elmas A (2000) When did the western Anatolian grabens begin to develop? Geol Soc Sp 173:353–384

Yolsal-Çevikbilen S, Taymaz T, Helvacı C (2014) Earthquake mechanisms in the Gulfs of Gökova, Sığacık, Kuşadası, and the Simav Region (western Turkey): neotectonics, seismotectonics and geodynamic implications. Tectonophysics 635:100–124. https://doi.org/10.1016/j.tecto.2014.05.001